PAPER • **OPEN ACCESS**

Development of a test rig for the study of gas-based nanofluids

To cite this article: Marco Milanese *et al* 2024 *J. Phys.: Conf. Ser.* **2893** 012110

Journal of Physics: Conference Series **2893** (2024) 012110 doi:10.1088/1742-6596/2893/1/012110

Development of a test rig for the study of gas-based nanofluids

Marco Milanese[1], Muhammad Faraz[1], Gianpiero Colangelo[1]* and Arturo de Risi[1]

[1] Department of Engineering for Innovation, University of Salento, Lecce, Italy

*E-mail: gianpiero.colangelo@unisalento.it

Abstract. Nanofluids, comprising nanoparticles suspended in conventional heat transfer fluids, reveal significant increase in thermal conductivity and convective heat transfer. This research article investigates the application of gas-based nanofluid in concentrated solar power plant (CSP) technologies. Traditional heat transfer fluids, like synthetic oil and molten salts, present limitations such as flammability, toxicity and operational temperature. In contrast, gas-based nanofluids show improved thermal and optical properties making them a promising alternative for high-temperature solar applications. In this research, an innovative open circuit test bench operating with gas-based nanofluid as heat transfer fluid is presented. Particularly, an open circuit test bench was designed for experimental analysis, incorporating a solar simulator to control sunlight intensity in a laboratory setting. A theoretical model was developed based on solar simulator irradiance, and numerical analysis was conducted. Nanofluids containing CuO nanoparticles exhibited an optimal extinction distance within a few centimeters at a volume concentration of 0.50%. Besides, also the temperature increase achievable with this concentration of nanoparticles is compatible with various thermal and electrical power generation applications.

1. Introduction

Today, modern nanotechnology enables the production of nanometer-sized metallic and nonmetallic particles, which exhibit unique mechanical, optical, electrical, thermal, and magnetic properties. Nanofluids, synthesized by suspending nanoparticles, typically less than 100 nm in size within conventional heat transfer fluids like water, oil, ethylene glycol, or air, are a prime example of this innovation. When these nanoparticles are uniformly dispersed and stably suspended in the base fluid, even in small amounts, they significantly enhance the thermal properties of the fluid.

The term "nanofluid" was first introduced by Choi [1] to describe a new class of heat transfer fluids based on nanotechnology. Since then, scientists and engineers have made significant strides in thermal study, discovering unexpected thermal properties, proposing new devices, developing unconventional models, and identifying unusual development opportunities such as smart coolants for computers or safe coolants for nuclear reactors.

Maxwell proposed the idea of improving heat transfer by adding solid particles to fluid [2]. This enhances the fluid thermal conductivity since solids normally conduct heat much better than fluids. Maxwell's concept is old, but the innovation with nanofluids lies in using nanoscale

particles, creating a stable, highly conductive suspension that avoids these issues, as gravity's effects are negligible, preventing erosion, deposits, and blockages.

The interest in using nanofluids in solar energy systems, especially in Concentrated Solar Power (CSP) technologies like Parabolic Trough Collectors (PTCs), is rapidly growing. Traditional heat transfer fluids such as synthetic oil and molten salts have limitations, including flammability, toxicity, and operational temperature constraints [3]. Gas-based nanofluids, which combine gases (e.g., air, nitrogen, helium, argon) with nanoparticles, represent a promising alternative. These nanofluids enhance the absorption of solar energy directly within the fluid and significantly increase the heat transfer surface area compared to conventional receivers. Research indicates that incorporating nanoparticles into these fluids can vastly improve their optical properties and efficiency, offering a potentially superior solution for high-temperature heat transfer in solar power plants [4-7].

The introduction of nanofluids as a heat transfer fluid makes it possible to overcome the limitations of synthetic oil and molten salts. Compared to base fluid, nanofluid exhibits high thermal conductivity and convective heat transfer coefficient [8,9]. Moreover, in the presence of nanoparticles, most nanofluids show notable optical properties such as a high absorption coefficient of solar radiation. High-temperature solar systems, that use gas-particle suspensions to absorb concentrated sunlight, have been studied for heating gases, both to drive turbines for electricity and to carry out suitable chemical reactions. In this way, Hunt [10] proposed to use a small particles heat exchange receiver to heat a working gas in a solar receiver to a high temperature for powering a gas turbine. Abdelrahman et al. [11] and Oman and Novak [12] have studied suspensions of nanometric solid particles in gases (particularly spherical particles of graphite), demonstrating that they have interesting selective absorption properties, whereas the emissivity in the IR range is low.

Miller and Koenigsdorff [13,14] have studied a large chamber filled with particle suspension and open on one side to admit solar radiation and found a fairly low dependence on the particle's size. They demonstrated that the system built on the megawatts-size could reach very high efficiency. Bertocchi et al. [15] proposed an experimental evaluation of a solar particle receiver, where concentrated solar radiation was converted into thermal energy. The proposed heat transfer fluid was a mixture of a gas with absorbing sub-micrometer carbon particles. Particularly, they have shown that the estimated radiation-to-thermal energy conversion efficiency could be higher than 80%, at temperatures above 1700 K.

The above-described results encourage the use of gas-based nanofluid to absorb solar radiation. At present, the study of gas-based nanofluids is still at an early stage, and no test rig for studying the characteristics of this type of nanofluids are described in the literature. Therefore, in this paper, an innovative open-circuit test bench, operating with gas-based nanofluid as heat transfer fluid is presented.

2. Open circuit test bench

Figure 1 shows a schematic of the open circuit test bench that has been designed in the present work.

The open-circuit test bench works by using a compressor to draw in and compress clean air. Nanopowders are then added through a hopper, and the resulting nanofluid is heated in an optical test rig, equipped with 2 optical windows (an upper window for incident radiation input and a lower one for measurement of residual unabsorbed radiation). The powders can be reused, thanks to a filtering system.

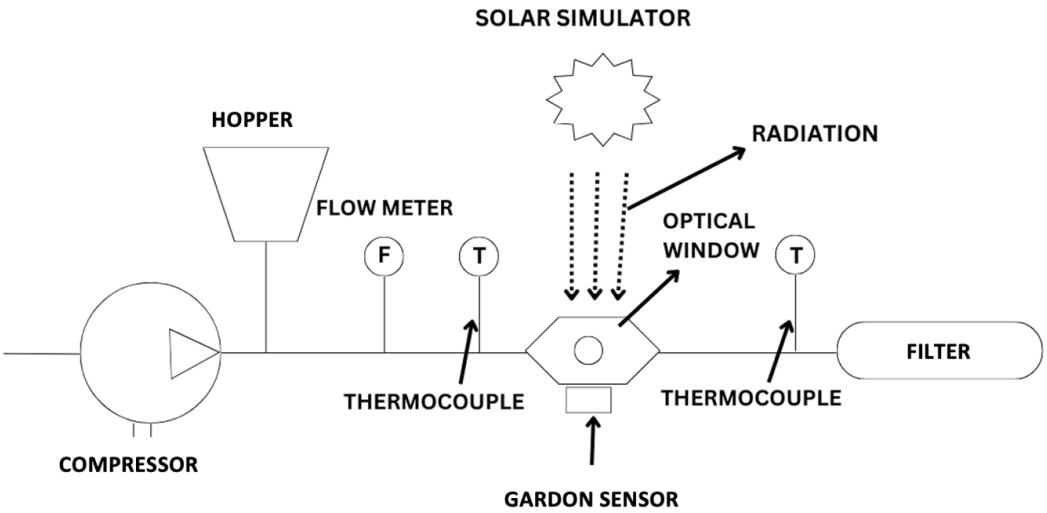

Figure 1: Schematic of an open circuit test bench

The key advantages of this system include always using clean air for the compressor and the ability to easily adjust the concentration of powders. However, it needs to be stopped periodically to clean up the filter and refill the hopper.

For particle heating, a solar simulator is used. Particularly, this method is based on special lamps to reproduce the intensity of concentrated sunlight in the laboratory. To handle the heat and maintain transparency, the nanofluid flows through a quartz tube. This setup ensures effective heating by the simulated sunlight, allowing the study of the behavior of gas-based nanofluids under conditions similar to real solar radiation. Additionally, a second optical window and a Gardon sensor are used to measure light absorbed by the nanoparticles, and a filter is added to slow the flow and collect powders. This comprehensive setup will enable a complete study of gas-based nanofluids' behavior when heated by solar radiations.

2.1. High-flux solar simulators

In the last few years, several studies have been carried out on concentrating solar thermal and thermochemical applications. These studies can be further enhanced by means of high-flux solar simulators (HFSS), since they allow the development of experimental tests under controlled irradiance conditions, regardless of sunshine. Therefore, in this work, the data related to a high-flux solar simulator (Figure 2), capable of reaching levels of irradiance higher than 100 W/cm^2 (1000 suns), have been used to design the test bench [16].

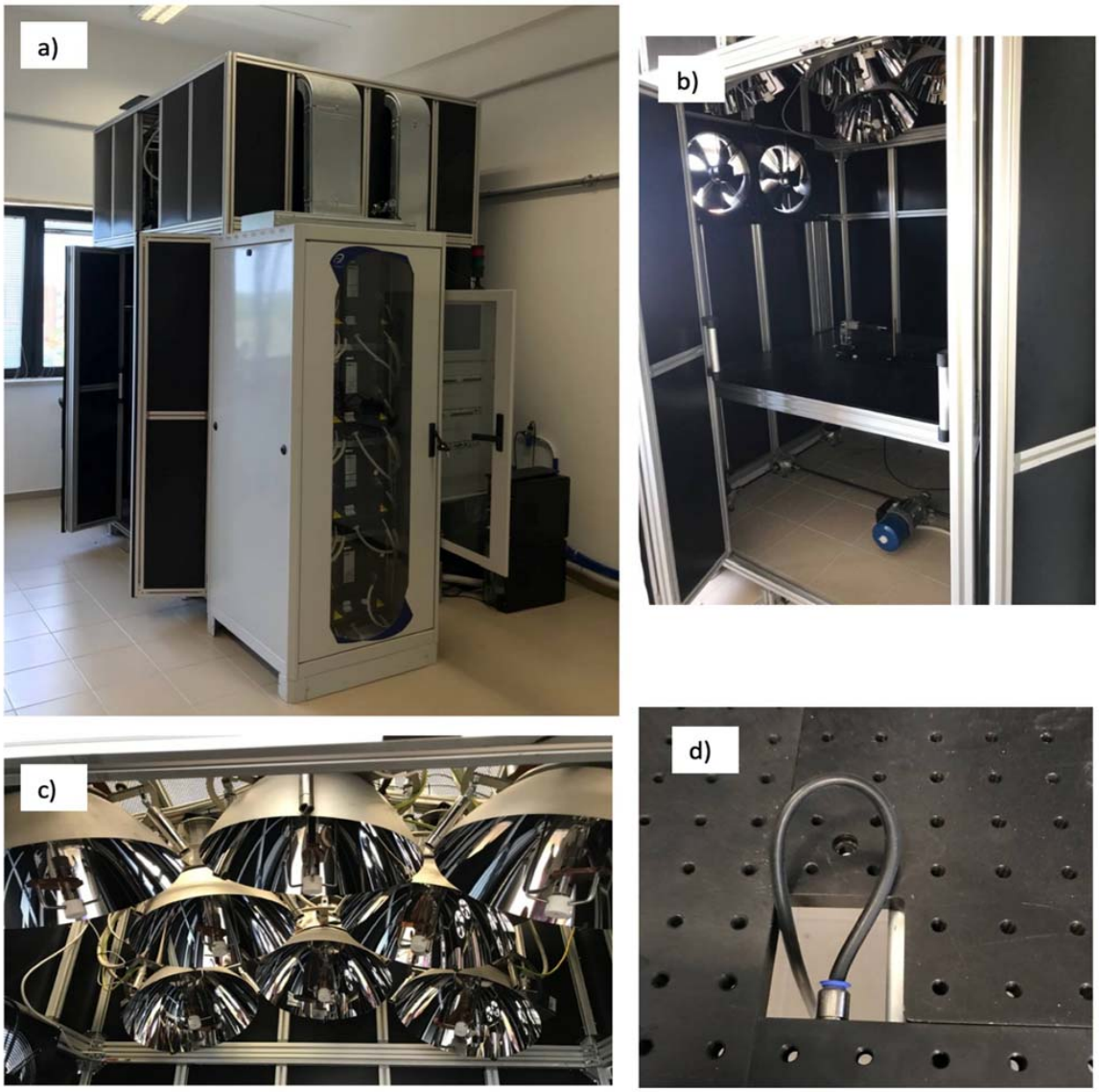

Figure 2: Pictures of the HFSS: (a) overall view; (b) inside view; (c) detail of the lamps; (d) detail of the chilled mobile optical bench

This solar simulator is composed of 8 ellipsoidal specular reflectors, arranged face-down on a horizontal plane, in order to irradiate from the upper side any system requiring the simulation of concentrated solar radiation; differently from other HFSSs described in the scientific literature, in which light radiation propagates laterally, this configuration allows the avoidance of any distortion of fluid-dynamic or convective phenomena within the system under investigation.

Finally, the HFSS has been characterized, measuring a maximum irradiance of 120 W/cm^2 and a maximum temperature of 1007 °C; these values will be enough to develop experimental tests on lab-scale thermal and thermochemical solar applications.

3. Numerical Simulation

The main core of the new test bench is a test rig equipped with two quartz windows for input of incident radiation and measurement of absorbed radiation. In order to design the new optical test rig, a numerical simulation was developed based on two models: an optical and a thermodynamic model described below.

3.1. Optical model

Light is attenuated when it travels through a medium as a result of absorption and scattering phenomena [17,18]. The optical model neglects the effect of quartz windows.

Figure 3 shows the schematic of optical model with incident, scattered, absorbed and passing radiation through a transparent tube crossed by a nanoparticle flow.

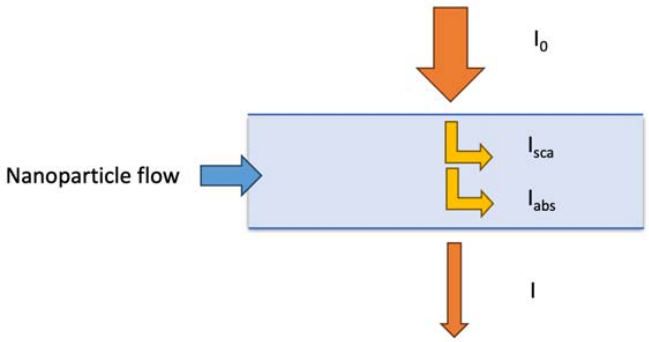

Figure 3: Schematic of optical model

According to de Risi et al. [19] and Hulst et al. [20], let consider the relationship between the intensity of incident light I_o [W/m^2] and the intensity of scattered light I [W/m^2] at a point located a distance z [m] from the particle. The wave number k [m^{-1}] is defined as $k=2\pi/\lambda$, where λ [m] is the wavelength in the surrounding medium. The intensity of scattered light I must be proportional to the intensity of incident light I_o and inversely proportional to the square of the distance z from the particle, and can be expressed as:

$$I = \frac{I_o F(\theta,\varphi)}{k^2 z^2} \tag{1}$$

In Eq. (1), $F(\theta,\varphi)$ is a dimensionless function of the direction, but not of z. It also depends on the particle direction relative to the incident wave, as well as the on the state of polarization for incident wave. The scattered light intensity is proportional to the intensity of the incident light, with the total scattered energy in all directions equal to the energy of the incident wave that fell on the area C_{sca}. Thus, we have:

$$C_{sca} = \frac{1}{k^2}\int F(\psi,\varphi)d\omega \tag{2}$$

In Eq. (2) $d\omega = sin\psi d\psi d\varphi$ represents the element of solid angle, and the integral is performed over all directions.

According to definition, if the absorbed energy of the particle is equal to the energy incident on the surface area C_{abs}, and C_{sca} is the energy incident area equal to energy removed from the incident ray, then by law of conservation of energy:

$$C_{ext} = C_{sca} + C_{abs} \tag{3}$$

the term C_{ext}, C_{sca} and C_{abs} in Eq. (3) are the optical cross-section of the particles [m²]. Further the following Eq. (4)(5)(6) shows the efficiency factors for extinction, scattering and absorption, that can be written as:

$$E_{ext} = \frac{C_{ext}}{G} \tag{4}$$

$$E_{sca} = \frac{C_{sca}}{G} \tag{5}$$

$$E_{abs} = \frac{C_{abs}}{G} \tag{6}$$

Where the term G [m²] is the cross-section of nanoparticle. Therefore, Eq. (3) can be written as:

$$E_{ext} = E_{sca} + E_{abs} \tag{7}$$

For spherical particle with a diameter smaller than the wavelength of incident light, the terms C_{sca} and C_{abs} can be rewritten as, according to [19]:

$$C_{sca} = E_{sca}G = \frac{8}{3}\chi^4 \left|\frac{m^2-1}{m^2+2}\right|^2 \pi a^2 \tag{8}$$

$$C_{abs} = E_{abs}G = -4\chi^4 Im\left\{\frac{m^2-1}{m^2+2}\right\}\pi a^2 \tag{9}$$

Here a is particle radius [m], m is the complex refractive index of the particle that can be written as *(m = u-iu')*, and χ can be written as $\chi = ka$, the product of wave number k and particle radius a.

At this stage, the extinction cross-section can be calculated as a sum of absorption and scattering cross-sections. The extinction coefficient is defined as:

$$\gamma = NC_{ext} \tag{10}$$

Where N is the number of particles per unit volume in the nanofluids. Using this equation and Beer Lambert Law [21] the extinction distance (d_{ext}) can be calculated by solving:

$$t = \frac{I}{I_\circ} = e^{-\gamma_{ext}d_{ext}} = e^{-NC_{ext}d_{ext}} \tag{11}$$

In Eq.11 t is attenuation coefficient. In this study, the extinction distance was calculated by setting attenuation coefficient equal to 0.01.

In this work, the optical model was applied by considering nanoparticles of CuO, whose refractive index is shown in Figure 4.

3.2. Thermodynamic model

The thermodynamic model that enables a comprehensive analysis of nanofluid properties and flow characteristics is described below.

First, the volumetric flow rate of the nanofluids is determined using Eq. 13. The initial relationship for volumetric flow rate, $\dot{Q}$ [m³/s], is:

$$\dot{Q} = \upsilon A \tag{12}$$

Where υ [m/s] represents the particle velocity and A [m²] is the cross-section area of the optical test rig.

$$\dot{Q} = \upsilon \frac{d^2\pi}{4} \tag{13}$$

The air density, ρ_{air} [kg/m³], is calculated using the ideal gas law in Eq.14:

$$\rho_{air} = \frac{p}{RT} \tag{14}$$

Where p [Pa] is the pressure, R [J/kg K] is the specific gas constant for air and T [K] is the temperature.

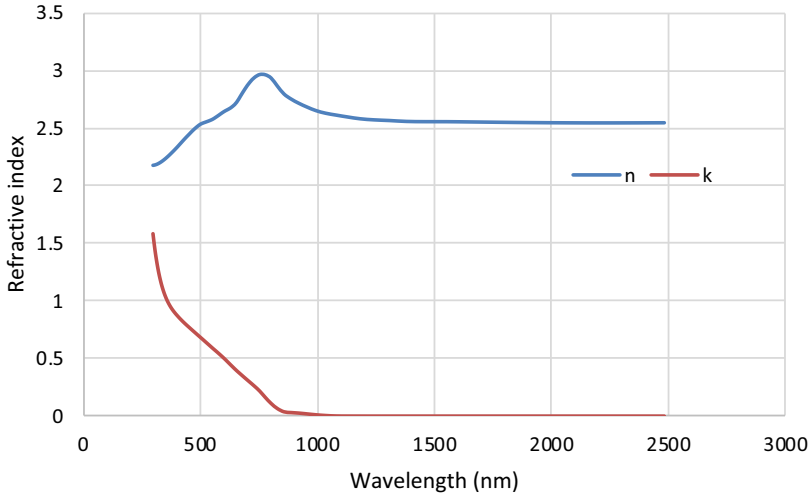

Figure 4: Refractive index of CuO

To determine the density of the gas-based nanofluids, Eq.15 is applied:

$$\rho_{NF} = \rho_{air}(1 - \Phi) + \rho_{NP}\Phi \quad (15)$$

In this equation ρ_{NF} [kg/m³] represents the density of nanofluids, ρ_{NP} [kg/m³] is the nanoparticle density and Φ is the volumetric concentration of nanoparticles in the fluid. This equation accounts for the contribution of both the base fluid and the nanoparticles to the overall density of the nanofluids.

The specific heat capacity of the nanofluid represents an important thermal property and is calculated using Eq.16:

$$C_{p,NF} = (1 - \Phi)C_{p.air} + \Phi C_{p.NP} \quad (16)$$

Here $C_{p,NF}$ [J/kg K] is the specific heat capacity of nanofluids, $C_{p,air}$ [J/kg K] is the specific heat capacity of air and $C_{p,NP}$ [J/kg K] is the specific heat capacity of nanoparticles. This equation reflects the weighted contributions of the air and the nanoparticles to the overall specific heat capacity of the nanofluid.

Finally, the mass flow rate of the nanofluid is derived using Eq.17.

$$\dot{m}_{NF} = \rho_{NF}\dot{Q} \quad (17)$$

Where $\dot{m}_{NF}$ [kg/s] is the mass flow rate and $\dot{Q}$ is the volumetric flow rate from Eq.13.

By measuring the nanofluid flow rate and the inlet and outlet temperatures, T_{in} [K] and T_{out} [K], from the test rig, it is possible to calculate the thermal power input. This data finally can be compared with incident radiation through the optical window of area A_w [m²], in order to make a thermodynamic balance of the system.

$$\dot{m}_{NF}C_{p,NF}(T_{out} - T_{in}) = (I_0 - I)A_w \quad (18)$$

These equations are essential for understanding the flow characteristics and its thermal behavior.

4. Discussion of results

The design of the optical test rig is based on:
- the experimental optical characterization of the HFSS;
- the numerical simulations through the optical model.

Figure 5 shows the maximum irradiance reached on the workbench when all lamps are switched on, at 40% of power (1600 W) and at maximum power of 3600 W, respectively.

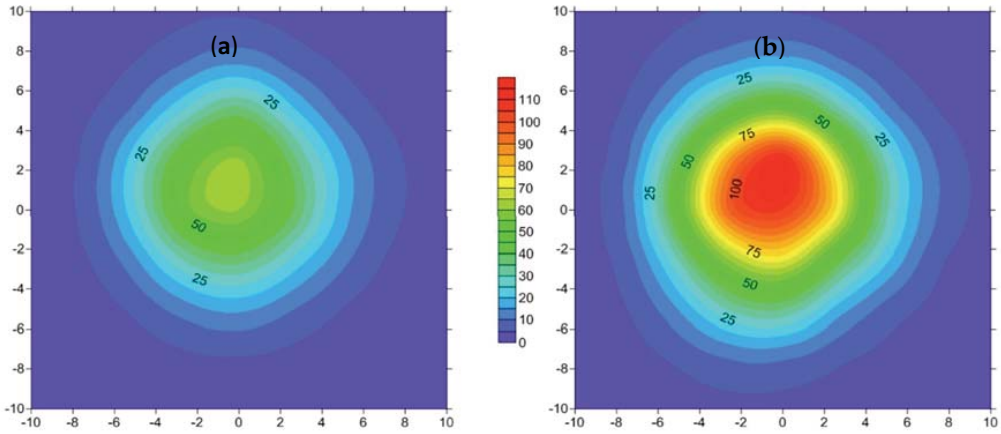

Figure 5: Irradiance [W/cm²] reached with all lamps switched on; (a) 40% of power (1600 W); (b) 80% of power (3600 W); the coordinates are expressed in cm from the center of the workbench; the colormap scale is referred to both graphs

Taking these points into account, a theoretical model to test the thermal and optical properties of the nanofluids at high temperature has been developed.

4.1 Optical properties of the nanofluids

The optical model was applied by considering nanoparticles of CuO, whose refractive index is shown in Figure 4.

Figure 6 shows the extinction distance for a CuO nanofluid as a function of incident wavelength for particles concentration in the range between 0.10% and 3.0%.

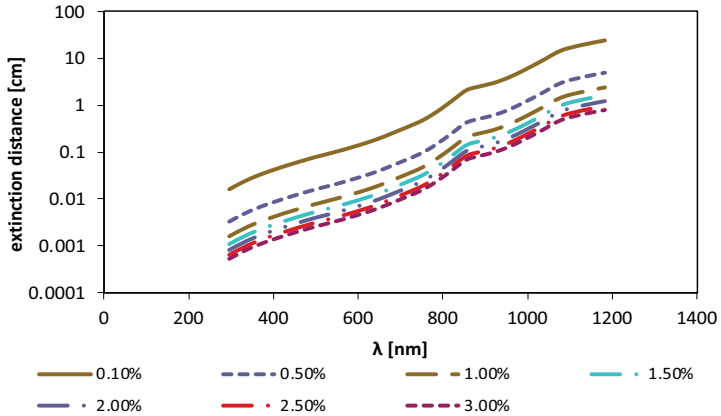

Figure 6: Extinction distance for CuO nanofluid at different concentrations of nanoparticles

As it can be observed, a CuO nanoparticles volume concentration equal to 0.5% was found to be enough to absorb the solar radiation (up to 1200 nm) passing through the optical window, within a distance of few centimeters.

According to the experimental measurements of Figure 5 and the numerical results of Figure 6, the optical test rig has been designed.

It is composed by:

- an upper optical window through which incident radiation enters;
- a lower optical window for the measurement of residual radiation (fraction of radiation not absorbed by the nanofluid);
- a square-shaped tube for supporting the optical windows;
- two inlet and outlet ducts.

A schematic of the optical test rig is shown in Figure 7.

The size of the optical windows (diameter equal to 4 cm) was set according to the irradiance maps shown in Figure 5.

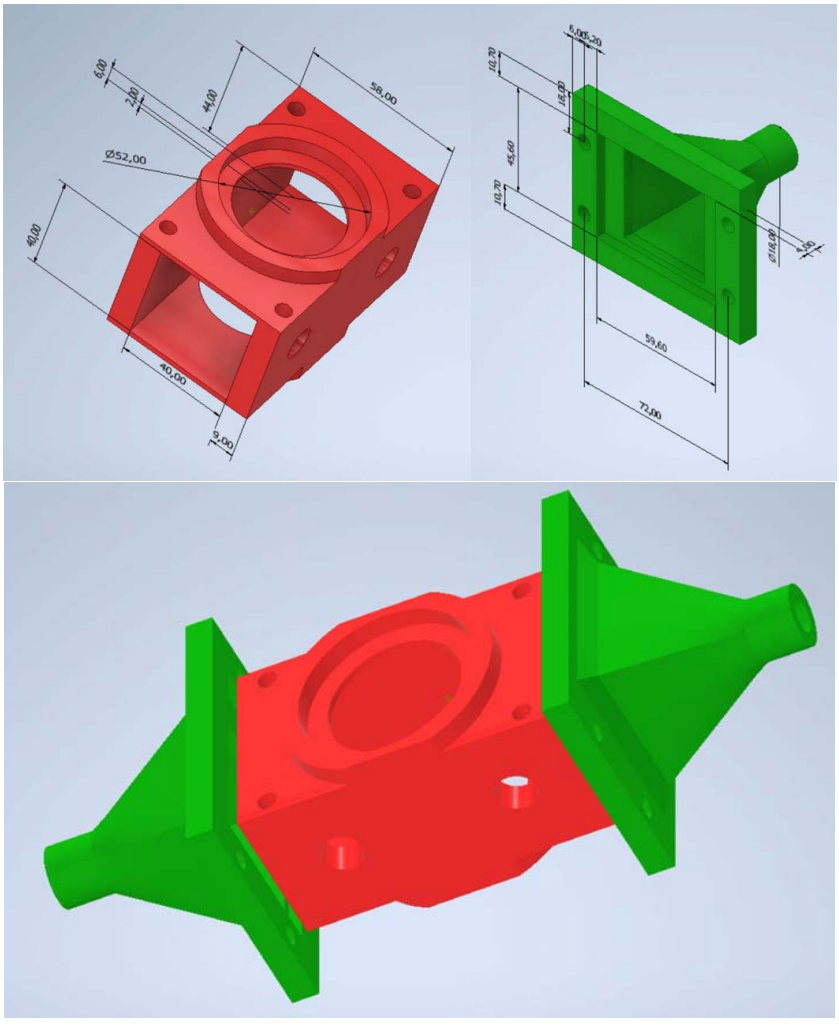

Figure 7: Schematic of the optical test rig (dimensions in mm)

In accordance with the extinction distance, shown in Figure 6, and the geometry of the optical test rig, shown in Figure 7, by means of the above-described thermodynamic model, the rise in temperature achievable with an incident radiation of 100 W/cm² was calculated. These results are shown in Figure 8 for different volume particle concentrations of CuO nano particles, ranging from 0.50% to 3.00%.

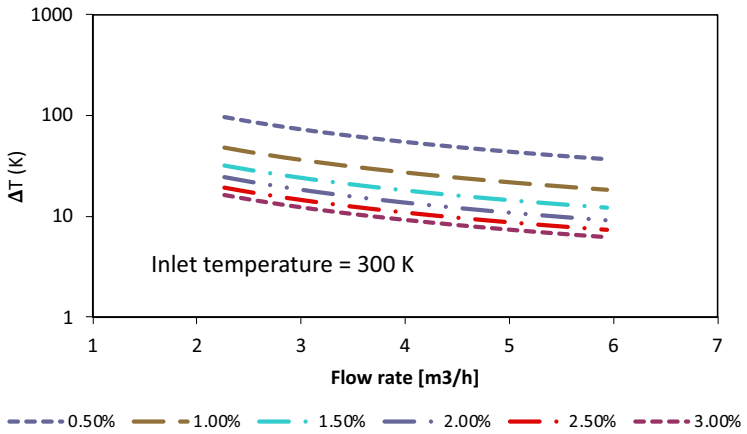

Figure 8: Increase in temperature between inlet and outlet of the holder as a function of nanofluid flow rate and CuO nanoparticles volume concentration.

It can be observed that, at 0.50% particle concentration of CuO, the nanofluid revealed a maximum temperature increase of about 100 K. Assuming the implementation of several transitions in a concentrating system, this value can be compatible with various thermal and electrical power generation applications.

5. Conclusion

In this work, an innovative test bench was simulated and designed to test gas-based nanofluids as heat transfer fluids, which absorb radiation from a solar simulator. Particularly, a numerical model was developed, taking into account the geometrical, thermal, and fluid dynamics aspects of the test bench. The numerical results demonstrated that gas-based nanofluids could be an effective alternative to conventional fluid for high-temperature applications, such as synthetic oil or molten salt, which have encountered various problems in existing plants. Simulation of the gas-based nanofluid absorption spectrum with CuO nanoparticles indicated a maximum extinction distance of a few centimeters at a volume concentration of 0.50%. Besides, also the temperature increase achievable with this concentration of nanoparticles is compatible with various thermal and electrical power generation applications.

Acknowledgments

This work was funded by the European Union – Next Generation EU - Italian NRRP, Mission 4, Component 2, Investment 1.1 “Fund for the National Research Program and Projects of Significant National Interest (PRIN)” (Directorial Decree n. 1409/2022) “PRIN 2022 PNRR” –Title

of the Project: Gases with nanoparticles as working fluid for CSP technologies (nanoCSP), Project Code: P2022RAN9Z, CUP F53D23009840001. This work reflects only the authors' views and opinions, neither the Ministry for University and Research nor the European Commission can be considered responsible for them.

References

[1] Choi S U and Eastman J A 1995 Enhancing thermal conductivity of fluids with nanoparticles (No. ANL/MSD/CP-84938; CONF-951135-29) Argonne National Lab. (ANL), Argonne, IL (United States).
[2] Maxwell J C 1873 A treatise on electricity and magnetism (Vol. 1). Oxford: Clarendon Press.
[3] Manzolini G, Bellarmino M, Macchi E and Silva P 2011 Solar thermodynamic plants for cogenerative industrial applications in southern Europe *Renewable Energy 36*(1), 235-243.
[4] Abdelrahman P, Fumeaux P and Suter P 1979 Study of solid-gas suspension used for direct absorption of concentrsated solar radiation *Solar Energy* 22, 45-48.
[5] Oman J and Novak P 1996 Volumetric Absorption in Gas-Properties of Particles and Particle-Gas Suspension *Solar Energy* 56(6) 597-606.
[6] Miller F J and Koenigsdorff R W 1991 Theoretical-analysis of a high-temperature small-particle solar receiver *Solar Energy Materials* 24, 210-221.
[7] Miller F J and Koenigsdorff R W 2000 Thermal modeling of a small-particle solar central receiver *Journal of Solar Energy Engineering* 122, 23-29.
[8] Kakaç S and Anchasa P 2009 Review of convective heat transfer enhancement with nanofluids *International Journal of Heat and Mass Transfer* 52, 3187-96
[9] Buongiorno J 2010 Convective transport in nanofluids *Journal of Heat Transfer* 128(3) 240.
[10] Hunt A J 1978 Small particle heat exchanger *Lawrence Berkeley National Laboratory*.
[11] Abdelrahman P, Fumeaux P and Suter P 1979 Study of solid-gas suspension used for direct absorption of concentrated solar radiation *Solar Energy* 22, 45-8.
[12] Oman J and Novak P 1996 Volumetric absorption in gas-properties of particles and particle-gas suspension *Solar Energy* 56(6), 597-606.
[13] Miller F J and Koenigsdorff R W 1991 Theoretical-analysis of a high-temperature small particle solar receiver *Solar Energy Materials* 24, 210-21.
[14] Miller F J and Koenigsdorff R W 2000 Thermal modeling of a small-particle solar central receiver *Journal of Solar Energy Engineering* 122, 23-9.
[15] Bertocchi R, Karni J and Kribus A 2004 Experimental evaluation of a non-isothermal high temperature solar particle receiver *Energy* 29, 687-700.
[16] Milanese M, Colangelo G and de Risi A 2021 Development of a high-flux solar simulator for experimental testing of high-temperature applications. *Energies 14*(11), 3124.
[17] Milanese M, Colangelo G, Cretì A, Lomascolo M, Iacobazzi F and de Risi A 2016 Optical absorption measurements of oxide nanoparticles for application as nanofluid in direct absorption solar power systems – Part I: Water-based nanofluids behavior *Solar Energy Materials & Solar Cells* 147, 315–320.
[18] Milanese M, Colangelo G, Cretì A, Lomascolo M, Iacobazzi F and de Risi A 2016 Optical absorption measurements of oxide nanoparticles for application as nano uid in direct absorption solar power systems– Part II: ZnO, CeO2, Fe2O3 nanoparticles behavior *Solar Energy Materials & Solar Cells* 147, 321–326.
[19] De Risi A, Milanese M and Laforgia D 2013 Modelling and optimization of transparent parabolic trough collector based on gas-phase nanofluids *Renewable Energy* 58, 134-139.
[20] Hulst H C and van de Hulst H C 1981 Light scattering by small particles *Courier Corporation*.
[21] Ricci R W, Ditzler M and Nestor L P 1994 Discovering the beer-lambert law *Journal of chemical Education* 71(11), 983.